

DYNAMIC BEAM ATTENUATOR

May 9, 2012

Team

Clara Chow – BSAC

Katherine Lake – Communicator

Ashley Mulchrone – BWIG

Michael Scherer – Team Leader

Clients

Dr. Chuck Mistretta

Tim Szczykutowicz

Department of Medical Physics

Advisor

Professor Paul Thompson

Adjunct Professor, Biomedical Engineering

ABSTRACT

In 2010, the *Journal of Radiation Research* estimated that over 70 million Computed Tomography (CT) scans, using over 10,000 CT scanners, are performed in the US every year [1]. Since there is a small probability that CT scans will induce cancer, patient dose from each scan must be reduced. Current X-Ray CT employs a point source X-Ray generator that projects uniform radiation through the patient and is captured by the detector to produce a two-dimensional slice of a three-dimensional image. However, uniform beam intensity results in unequal noise distributions and patient over-exposure to radiation. In order to lower the patient dose and improve the image, the X-Ray intensity to certain parts of the patient can be selectively attenuated, or decreased, in both time and space. The image can be improved by increasing the signal to noise ratio through reducing X-Ray scatter and increasing noise uniformity.

One method to dynamically attenuate the X-Rays involves placing varying thicknesses of absorbing metal between the X-Ray source and the patient. Our team developed a device consisting of a parallel array of overlapping steel wedges. Linear servomotors drive the wedges in and out of the X-Ray field, changing the metal thickness between the source and the patient. An algorithm generates servo drive commands in real time based on desired attenuation. Simulations have shown that this device could decrease X-Ray dosage by up to 43%, reduce scatter by up to 79%, and improve noise uniformity by 9% when compared to a scan with no dose reduction methods used. After fabrication, the device was validated for position and attenuation accuracy and a linear relationship was obtained between motor input and wedge position. Measurements showed that a wedge could be reliably positioned within 180 microns of the determined linear relationship, exceeding our client's requirements. Repeatability was also tested with a CT scanner which showed a $0.12 \pm 0.079\%$ difference in attenuation between images.

TABLE OF CONTENTS

ABSTRACT	2
INTRODUCTION	4
CLIENT DESCRIPTIONS	4
X-RAY COMPUTED TOMOGRAPHY	4
CURRENT METHODS	6
DESIGN OVERVIEW	7
PREVIOUS PROTOTYPE	8
DESIGN CRITERIA	8
MATERIALS	9
METHODS OF ACTUATION	12
ADDITIONAL DESIGN CONSIDERATIONS	13
FINAL DESIGN	15
TESTING	16
POSITIONAL ACCURACY AND PRECISION TESTING USING CALIPERS	17
POSITIONAL ACCURACY AND PRECISION TESTING USING CT SCANNER	18
ERGONOMICS	20
ETHICAL CONSIDERATIONS	20
FUTURE WORK	20
TESTING	20
PATENTING	20
MARKETING	21
REFERENCES	22
APPENDIX A – MATLAB CODE	25
APPENDIX B – PROJECT DESIGN SPECIFICATIONS	27
APPENDIX C: TECHNICAL DRAWINGS	29
APPENDIX D: TEST PLAN	31
INTRODUCTION	31
<i>Quality Objective</i>	31
1.1.1 <i>Primary Objective</i>	31
1.2.1 <i>Secondary Objective</i>	31
TEST METHODOLOGY	31
2.1 <i>Purpose</i>	31
2.2 TEST STRATEGIES	31
2.2.1 <i>Position Test using Calipers</i>	31
2.2.2 <i>Position Test using Computed Tomography (CT) Scanner</i>	32
APPENDIX E: JAVA CODE	33
SERVO CONTROLLER CLASS	33
TEST CODE GENERATOR CLASS	35
SAMPLE COMMAND FILE	36

INTRODUCTION

Client Descriptions

Dr. Charles Mistretta is a Professor of Medical Physics and Radiology for the University of Wisconsin School of Medicine and Public Health [2]. His group was responsible for the development of digital subtraction angiography (DSA) and his current research interests include the development of 4-dimensional DSA technology and dynamic beam attenuation (DBA) in X-Ray computed tomography (CT) scanning [3]. Dr. Mistretta is also an Affiliate Professor in the Biomedical Engineering department and holds a research partnership with the University of Wisconsin Biomedical Engineering Center for Translational Research [2]. He has published work in numerous peer-reviewed journals and has generated 33 US patents [3].

Timothy Szczykutowicz is a doctoral degree student in the Department of Medical Physics at the University of Wisconsin-Madison. He is working on the dynamic beam attenuator project under Dr. Mistretta. Some of his current work pertains to calculating the level of attenuation required to produce quality, clear images and to determining how to reconstruct the image after attenuation has dynamically altered the intensity of X-Ray photons. Siemens, a global electrical engineering company, is funding the DBA project and has also provided an Artis Zeego Multi-Axis C-Arm CT scanner to use in DBA research [4]. Siemens hopes to integrate DBA into next generation CT scanners to improve image quality and lessen the adverse effects of radiation exposure.

Our clients have proposed that we design a wedge-based X-Ray attenuating prototype for DBA research as well as the means to actuate the prototype.

X-Ray Computed Tomography

Until the later part of the 20th century, the primary method of imaging in medical diagnostics was X-Ray radiography. This method projects X-Rays from a generator that pass through the desired object (in medical circumstances, the patient), and are detected by a sensor opposite the source [5]. The variation in density and composition of the patient would correspond to the black and white contrast in the final X-Ray image [6].

In 1979, the Nobel Prize in Physiology for Medicine was awarded to Allan M. Cormack and Godfrey N. Hounsfield for their “development of the computer assisted tomography” [6].

The limitation that traditional X-Ray imaging posed was its inability to produce three-dimensional images. With the advent of X-Ray computed tomography, three-dimensional images could be produced—a breakthrough that would greatly improve diagnostic radiology [7]. The X-Ray CT employs a point-source X-Ray generator that projects X-Rays in a fan-shaped array through the patient. Figure 2 shows a conventional CT machine; the patient is inserted into the round opening and the scanning procedure commences. The X-Rays are detected by a detector on the opposing side [8]. A schematic of the relative positions of the patient, the X-Ray beam generator, and the X-Ray detector is shown in Figure 1. The number of X-Rays that pass through the patient are detected and used to construct planar images. Image slices are produced as the patient moves through the beams. These slices are then compiled to produce a three-dimensional image, allowing what would traditionally be generated as pixels in a two-dimensional scan to be generated as three-dimensional voxels [9]. These three-dimensional reconstructions are then used by a variety of medical personnel for diagnoses. The benefits of this type of imaging include the ability to perform procedures with real time visual streaming and the non-invasiveness of the overall procedure. The method, however, also carries the disadvantage of increased lifetime cancer risk for the patient due to exposure to high intensity X-Ray beams [10]. In addition, there are certain qualitative drawbacks to the current method of computed tomography; the most notable being low image quality caused by the lack of beam attenuation.



Figure 2: A conventional CT machine developed by General Electronics Healthcare [10].

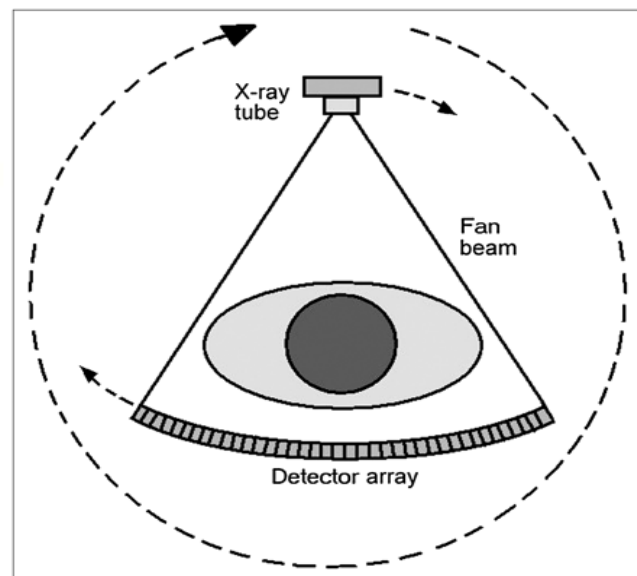


Figure 1: Schematic of a point-source-generated fan shaped X-Ray beam with a patient positioned between the beam source and the detector. No beam attenuation exists in this model [11].

Current Methods

One current shortcoming of X-Ray computed tomography is the use of a uniform incident beam despite the fact that the transmission through the patient varies significantly due to differences in tissue densities within the patient [11]. This results in a number of different problems. One problem is that a low, non-uniform signal-to-noise ratio can be a result of a non-attenuated, uniform beam; if the signal-to-noise ratio is too low or is non-uniform, a grainy and substandard image is produced. Also, because the beam is of a constant intensity, a sub-optimal distribution of X-Ray scatter occurs. If the beam were to be continually attenuated to account for the density and composition of the subject, fewer X-Rays would scatter, consequently resulting in a clearer final image [8]. Finally, significantly higher doses than necessary are administered to some regions and insufficient doses are administered to others [11].

X-Ray beam attenuation is one of the methods currently used to address these problems. X-Ray beam attenuation is defined as a reduction in X-Ray intensity; this reduction occurs after the X-Rays have been generated. One way to attenuate X-Ray beams is by using X-Ray tube modulation [12]. Concern about the amount of X-Ray exposure due to the high intensity beams necessary for diagnostic resolution led to the development of modulation of the X-Ray tube. This modulation is achieved by controlling the current in the X-Ray tube based on the necessary X-Ray beam intensity. The beams are either modulated based on preprogrammed predictive algorithms, or on continuous real-time feedback adjustments [13]. This is the primary method of reducing the high dosage of X-Rays that patients are exposed to without compromising the quality of the final images [14].

Static filters, such as the bowtie filter shown in Figure 3: Schematic of a point-source-generated fan shaped X-Ray beam with a bowtie filter positioned between the beam source and the patient. Passive beam attenuation exists in this model [21]., are also used in point-source-generated fan shaped X-Ray beam CT machines. This 'bowtie-shaped' component attenuates the X-Ray beams to a greater degree nearer to the outer

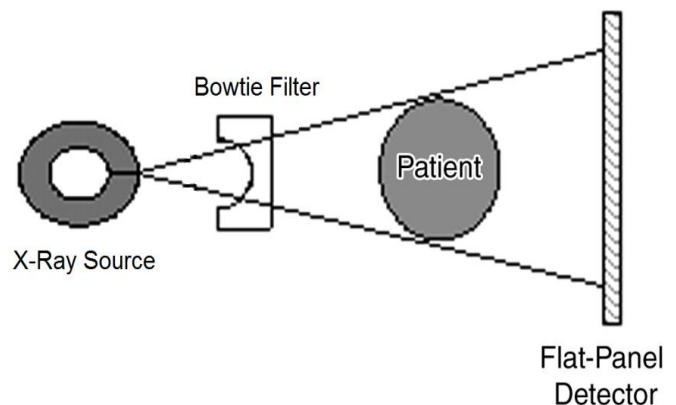


Figure 3: Schematic of a point-source-generated fan shaped X-Ray beam with a bowtie filter positioned between the beam source and the patient. Passive beam attenuation exists in this model [21].

edges of the X-Ray fan and less at the center of the bowtie, which corresponds to the areas of the patient with the greatest thicknesses. This filtration is designed to attenuate X-Rays based on the average shape in the human form and, besides X-Ray tube modulation, is one of the few methods of reducing X-Ray dosage during a CT scan.

DESIGN OVERVIEW

The goal of this device is to regulate the amount of X-Rays that each region of the patient receives at any given time. Our clients have proposed to do this using a series of paired wedges. By changing the amount of overlap and consequently the path length the beam must travel through, the amount of attenuation can be controlled throughout the duration of the scan. When the wedges are maximally overlapped, as seen in Figure 5, the X-Rays have to pass through a greater path length, which lowers the dosage delivered to the patient. However, if one wedge is slid away, as in Figure 5, the total thickness decreases and thus allows more X-Rays to pass. A series of wedge pairs placed between the X-Ray source and the patient could then adjust the total radiation passed to each region of a patient throughout the duration of a scan.

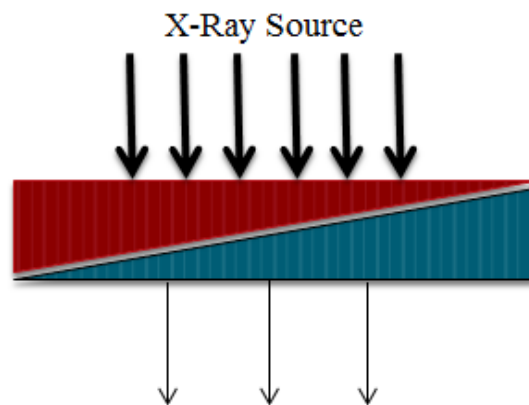


Figure 4: Overlapped wedges create high attenuation, allowing few X-Rays to pass through to the patient.

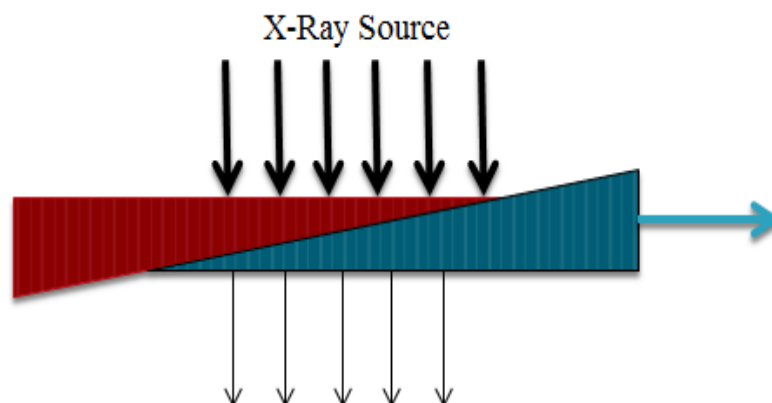


Figure 5: By sliding one wedge away, the amount of overlap decreases. This causes less attenuation and allows more X-Rays to pass.

Previous Prototype

The initial prototype, as seen in Figure 6, consists of a fixed top wedge-shaped plate and ten individual hand-actuated wedges. It was manufactured out of steel to the specifications shown in Appendix C: Technical Drawings. One wedge is linearly actuated by a 56.4 mm wide stepper motor, but the motor is significantly wider than the 17.5 mm wedge; this setup is not ideal as it does not allow easy actuation of small-width wedges without significant modification. We seek to create a device that actuates each wedge simultaneously along a linear path.

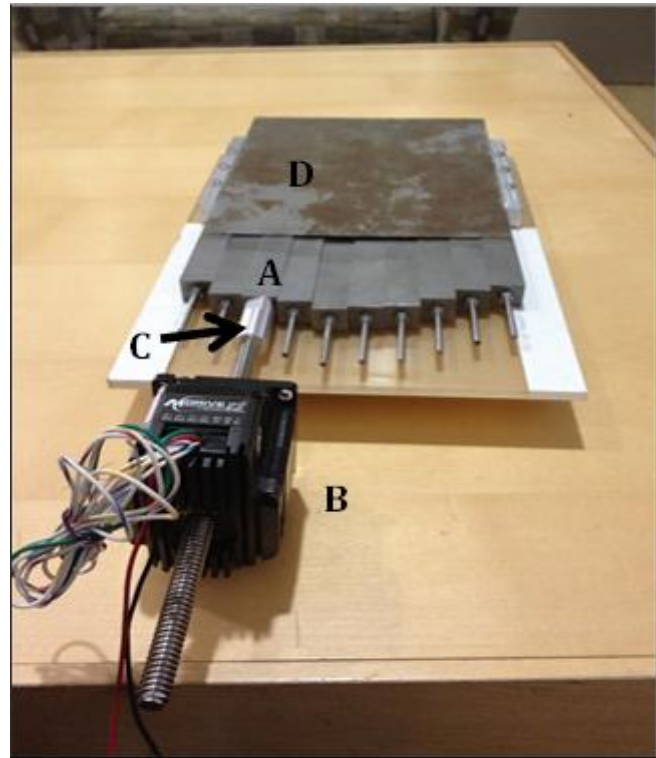


Figure 6: Actuated Prototype. The motor (B) drives the actuated wedge (A) inside the prototype housing (D) with a stroke length of up to 10 cm. The wedge is connected to the motor via an adaptor (C).

Design Criteria

The design must be accurate, compact, and resistant to X-Ray radiation. It cannot interfere with any part of the procedure or compromise the safety of the technician or the patient in any way.

First, the device needs to alter the strength of the X-Ray beam as a function of position for the duration of the Computed Tomography (CT) scan. In order to accomplish this, the actuator chosen must actuate the wedges to satisfy a minimum distance that encompasses approximately half of the area of the detector. This minimum actuation distance was determined to be 4 cm. The actuator must also move the wedges with a minimum movement increment of 1mm.

All components of the design shall be small enough to fit within the housing of the CT machine, which is approximately 27.94 centimeters. This is to demonstrate to Siemens, as a proof of concept, that this device could be constructed to scale to fit within the machine.

In addition, all parts should be resistant to damage by X-Ray radiation. The wedge material must be homogeneous in order to uniformly transmit X-Rays and correctly attenuate the

X-Ray beams. The wedges should also slide linearly with a low coefficient of friction. If implemented clinically, the device must have a life in service equal to that of the CT scanner.

Finally, the device should be safe and comfortable for both the medical personnel and the patient. No component should interfere with the execution of the procedure. The budget given by the client is approximately \$5000.

MATERIALS

In order to determine which material to pick for the final design, a few criteria were considered, including material thickness and beam hardening. Beam hardening is the uneven change in the X-Ray energy as it passes through a material, so that X-Rays with lower energies attenuate more than those with higher energies, which causes artifacts during CT image reconstruction.

MATLAB was used to calculate the minimum material thickness required to attenuate the X-Rays to the same level as 36 cm of soft tissue and 1 cm of bone. These values were chosen to model the chest and lung area, due to the large variation of ideal X-Ray dosages required between the sternum and the lungs. Equation 1 was used to match the amount of leaf material seen by the detector to the amount of patient material, where R is the specified thickness of soft tissue and bone, $\Omega(E)_k$ is the signal detected for a given spectrum at peak potential k , $w(E)$ is the detector energy, μ is the linear attenuation coefficients, and t_{tissue} and t_{bone} are soft tissue and bone thicknesses, respectively. In order to calculate the leaf thickness required, Equation 2 was used, and subsequently implemented into MATLAB (MATLAB code can be found in Appendix A.)

$$R_{t_{tissue}, t_{bone}} = \int dE \Omega(E)_k \cdot w(E) \cdot \exp(-t_{tissue} \cdot \mu(E)_{tissue} - t_{bone} \cdot \mu(E)_{bone}) \quad (1)$$

$$f(t_{leaf}) = \left| R_{t_{tissue}, t_{bone}} - \int dE \cdot \Omega(E)_k \cdot w(E) \cdot \exp(-t_{leaf} \cdot \mu(E)_{leaf}) \right| \quad (2)$$

Using these relationships, required leaf thicknesses for elements with atomic numbers 1 to 92 at 100 kVp were calculated; the results are shown in Figure 7. The energy specific attenuation values and mass densities for each material were obtained from NIST databases [22].

In **Error! Reference source not found.**, one can clearly see the wide range of hicknesses required, as based on the element selected. The peaks correspond to noble gases; a significant amount of gas is required to attenuate 36 cm of soft tissue and 1 cm of bone. The smallest leaf thickness is ideal, but other limitations, such as material availability and machinability, must also be considered.

Using these calculations, several materials were identified as potential wedge materials, including tungsten and copper. Research on materials currently used in radiation shielding and

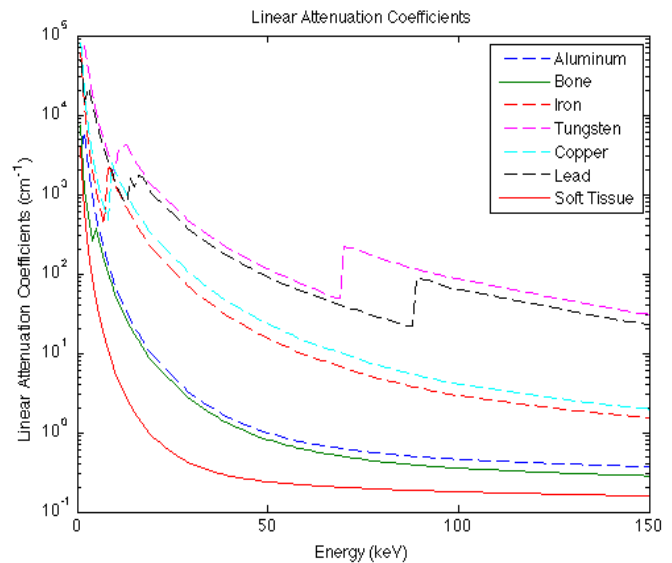
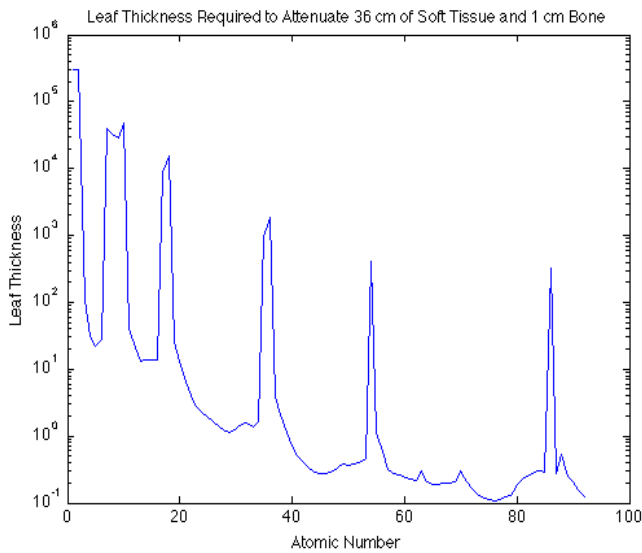


Figure 8: Leaf thickness required for elements with atomic number 1-92 to attenuate the same degree as 36 cm of soft tissue and 1cm of bone.

Figure 8: Linear attenuation coefficients as a function of energy for a variety of materials.

X-Ray technology revealed that lead, iron, and aluminum were also feasible materials to consider. These materials were then further analyzed by plotting the linear attenuation coefficients as a function of energy (Figure 8).

An ideal linear attenuation coefficient would be horizontal in this figure, or in other words, constant with respect to energy. However, as attenuation is a function of X-Ray photon energy, constantly attenuating materials do not exist. As a result, materials that have the lowest deviation from a constant mean energy are preferred. The data in Figure 8 show that tungsten and lead are the two materials that have the lowest deviation. All materials have k-edges, the jumps in linear attenuation coefficients at a characteristic X-Ray photon energy, but typically at much lower energies (less than 20 keV). A more constant mean energy within the middle of the diagnostic imaging X-Ray spectrum, 50 keV-100 keV, reduces beam hardening and therefore improves image quality.

To visually model the large differences in leaf thickness for the five materials considered, SolidWorks files of each material were created, and are shown in Figure 9. All dimensions were constant except for the heel thickness. Aluminum was scaled differently to improve comparability between heel thicknesses. These heel thicknesses were calculated by determining the amount of material required to match the signal produced by 36 cm of soft tissue and 1 cm of bone and range from 129.7 mm (Aluminum) to 1.2 mm (Tungsten).

After considering these simulations, a design matrix was constructed for five criteria: leaf thickness, beam hardening, machinability, cost, and heaviness (shown in Table 1). The values for each category were quantitatively determined from calculations and then normalized to a scale of 1 to 10, with the best material receiving a 10. Each criterion was then weighted according to importance so that the grand total was from 1 to 100. Both leaf thickness and beam hardening were calculated using the MATLAB simulations discussed earlier, and were

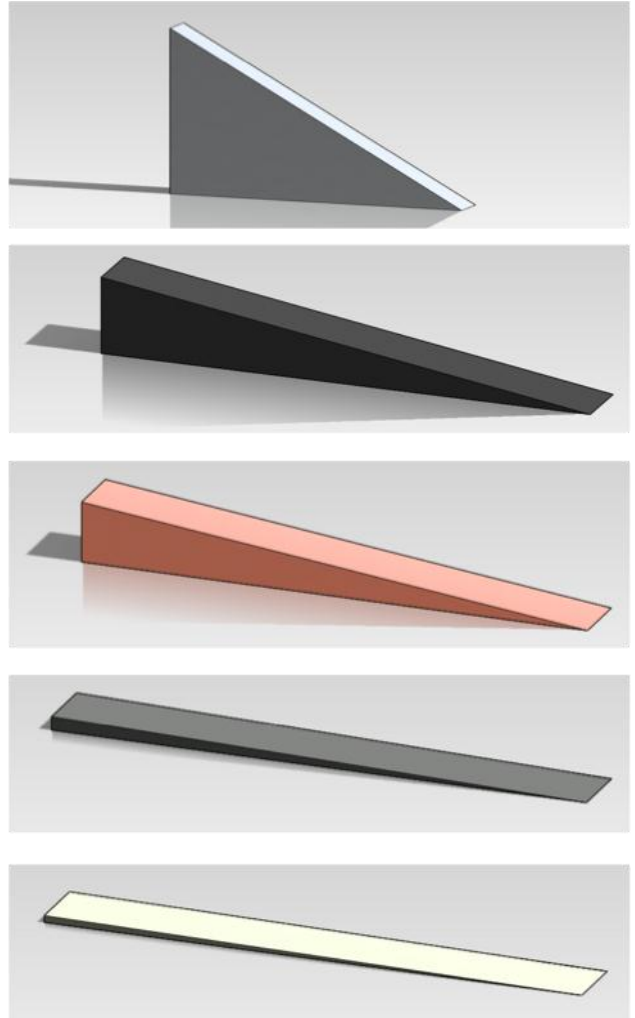


Figure 9: Leaf thicknesses for aluminum, iron, copper, lead, and tungsten, from top to bottom. Heel thicknesses were 129.7 mm, 16.3 mm, 11.4 mm, 2.5 mm, and 1.2 mm, respectively.

Table 1: Materials design matrix. Values were quantitatively determined and normalized to a scale from 1 to 10. Each criterion was then weighted so that the grand total was from 1 to 100.

Criteria	Weight	Lead	Tungsten	Copper	Iron	Aluminum
Leaf Thickness	4	4.91	10	1.06	0.74	0.09
Beam Hardening	2.5	7.96	10	7.36	7.4	8.23
Machinability	2	6	2	6	8	10
Cost	1	2.33	0.10	1.36	4.27	10
Weight/Heaviness	0.5	8.33	10	2.27	1.80	0.66
Total (out of 100)		58.0	74.1	37.1	42.6	51.3

given the largest weight because these two criteria are necessary for the proof of concept to work. Tungsten received the highest score in both these categories, because it had the smallest leaf thickness and the smallest beam hardening artifact. Machinability was considered next in importance. These values were determined based on rankings by a professional machinist, given the dimensions and leaf thicknesses required for each material. Aluminum was deemed easiest to machine, and tungsten the most difficult. The lowest weighted criteria were cost and heaviness, due to our relatively high budget and the consideration that the final design is only a proof of concept and will be stationary. However, it is important to note that heaviness will be a significant criterion to consider when implemented into the C-arm CT scanner since the C-arm will be rotating 270 degrees and a heavy design would cause balance problems. With these criteria, tungsten received the highest score, and was chosen for the preliminary design.

METHODS OF ACTUATION

After consulting with Erick Oberstar of the Mechanical Engineering Department at the University of Wisconsin-Madison, two main methods of wedge actuation were considered to properly actuate the attenuating wedges. The first method is a linear DC-Servomotor, which has the attractive feature of containing a position and speed feedback mechanism incorporated into the motor. This feature allows the motor to automatically correct for errors between the control signal and physical output. The best choice for this type of motor was determined to be the Series LM 1247 Linear DC-Servomotor with Analog Hall Sensors QUICKSHAFT Technology due to its stroke length, continuous force, precision, and size [15]. A Solidworks representation of a linear DC-Servomotor attached to an attenuating wedge is depicted in Figure 10. These motors present a problem, however, when considering the scalability and size constraints of the design. The Artis Zeego Multi-Axis C-Arm CT scanner's source enclosure, within which our prototype is designed to fit, has only a 25.4 square centimeter space to work within. If the linear servomotors were implemented, the motors themselves would require more space than the

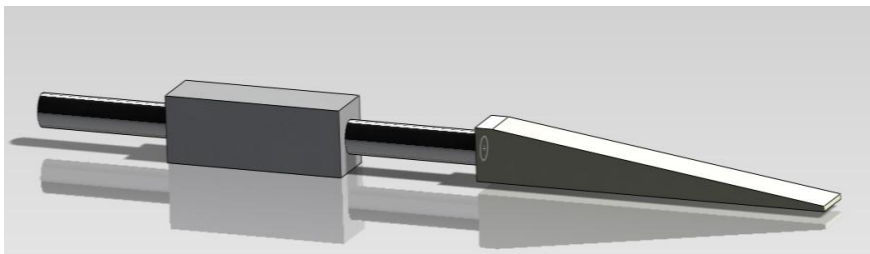


Figure 10: Solidworks representation of a linear DC-Servomotor attached to attenuating wedge.

attenuating wedges. To account for the increased space requirement, the wedge length must decrease. If the length of

the wedge were decreased while maintaining the heel height, an increase in the error would arise due to a steeper wedge angle. Alternatively, the wedge length and heel height could be decreased, but this would diminish the dynamic range of attenuation. Both of these outcomes are undesirable, so another form of actuation was considered.

The second possible method of actuation involves a rack and pinion system. The rack, or linear “gear” bar, would be affixed to the underside of the metal wedge, and be comprised of a minimally attenuating material such as plastic, nylon, or aluminum (Figure 11). The rack would create a baseline attenuation, but that value is easily accounted for during image reconstruction. The non-uniform surface due to gear pockets would also not cause a problem due to the “bucking grids” which are shaped like Venetian blinds and only allow radiation to be passed through to the detector that originated from the source, thus filtering out scattered beams [16]. The pinion, or circular gear, would be affixed to a brushless DC Servomotor, again provided by Micromo. Since these motors are also available with optional digital or analog hall sensors for position and velocity feedback, precision and position control are maintained. This design also allows for variable gear ratios to allow fine tuning of torque and speed with any given motor. The most attractive feature that differentiates this method of actuation from the linear motors is its compressed size. With a rack and pinion system, the majority of the area of the device can be utilized by the wedges, which maximizes dynamic attenuation range while minimizing error. For these reasons, the rack and pinion method of actuation should be utilized in the preliminary design.



Figure 11: Solidworks representation of rack and pinion system attached to attenuating wedge.

ADDITIONAL DESIGN CONSIDERATIONS

After our preliminary design was created, several changes were made to account for additional design constraints. One factor considered was the amount of tube loading, or the mAs increase, required to compensate for the minimum amount of metal in the X-Ray path. Since a part of the DBA will always be in the field of view, the amount of current must be increased in

order to obtain the same image without the baseline material in the path. The required increase in mAs, or tube current, was found to be several orders of magnitude higher than the scanner was capable of producing for tungsten and lead. Figure 12 shows the required mAs increase factor as a function of the atomic number. Tungsten and lead, with atomic numbers 74 and 82, respectively, have mAs increase factors over 1000, which is not feasible with current CT scanners. This eliminated tungsten and lead from possible metals. Iron and copper, the two remaining metal options, were evaluated more closely. The increase factor as a function of toe thickness is shown in Figure 13. This figure shows that smaller toe thicknesses and less tissue compensation require smaller mAs increases. Iron and copper reach above an mAs increase factor of 10 with 35 cm soft tissue compensation; according to our client, this increase factor was low enough to be feasible. Therefore, iron and copper were both found to be feasible materials for our design.

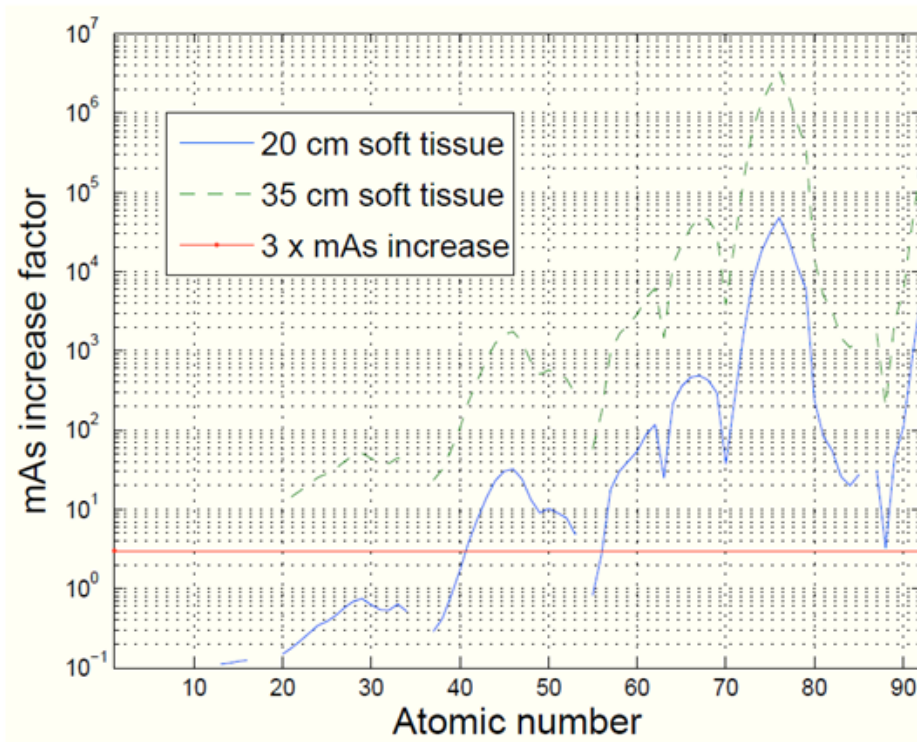


Figure 12: Required mAs increase as a function of atomic number for two thicknesses of soft tissue.

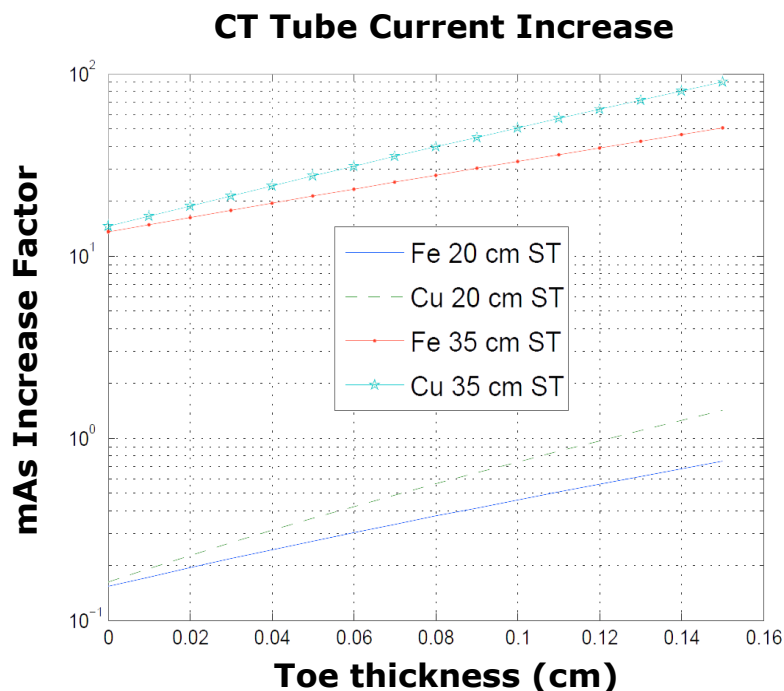


Figure 13: The necessary increase in mAs for copper and iron to compensate for the minimum amount of metal in the X-Ray path.

After the device material and size were selected, the original prototype was analyzed against the optimal device parameters. The original prototype uses steel wedges and a steel top plate; steel is mostly iron, and therefore the required mAs increase would not deviate sufficiently from the simulated mAs increases found for pure iron. The wedges were also long enough to ensure the required field of view would be attenuated. It was discovered that the prototype was sufficient for the final design.

FINAL DESIGN

The final design is shown in Figure 14, with alphabetized labels for identification. The entire device rests on a 30.5 x 61 cm acrylic base (A) and is comprised of ten 15 x 17.5 x 220 mm steel wedges (B) attached to two Firgelli L12-I and eight Firgelli L12-P 12 V linear servomotors (C). The two L12 -I servomotors can be directly integrated into the PhidgetAdvancedServo 8-Motor Controller (D) while each L12-P servomotor must be connected to a linear actuator controller board (E) before attachment to the motor controller. These two motor types were used because we were unable to purchase ten L12-I linear servomotors; an L12-P motor, in conjunction with a linear actuator control board, functions identically to the L12-I motor. Both linear servomotors have a stroke length of 100 mm and a 50:1 gear ratio to

ensure the wedges can traverse the dynamic range with sufficient velocity. They are connected to the steel wedges via couplers (F) that are screwed into each wedge and the couplers are attached to the servomotor by an aluminum screw cap. An acrylic track (not shown) is attached to the bottom of each wedge and sits in a straight cutout guide in the acrylic base. The track is used to ensure the wedges travel in a linear fashion. Graphite was added to decrease friction. A fixed 175 x 220 mm steel wedge (G) acts as the top wedge to ensure that the material thickness is uniform in the X-Ray path.

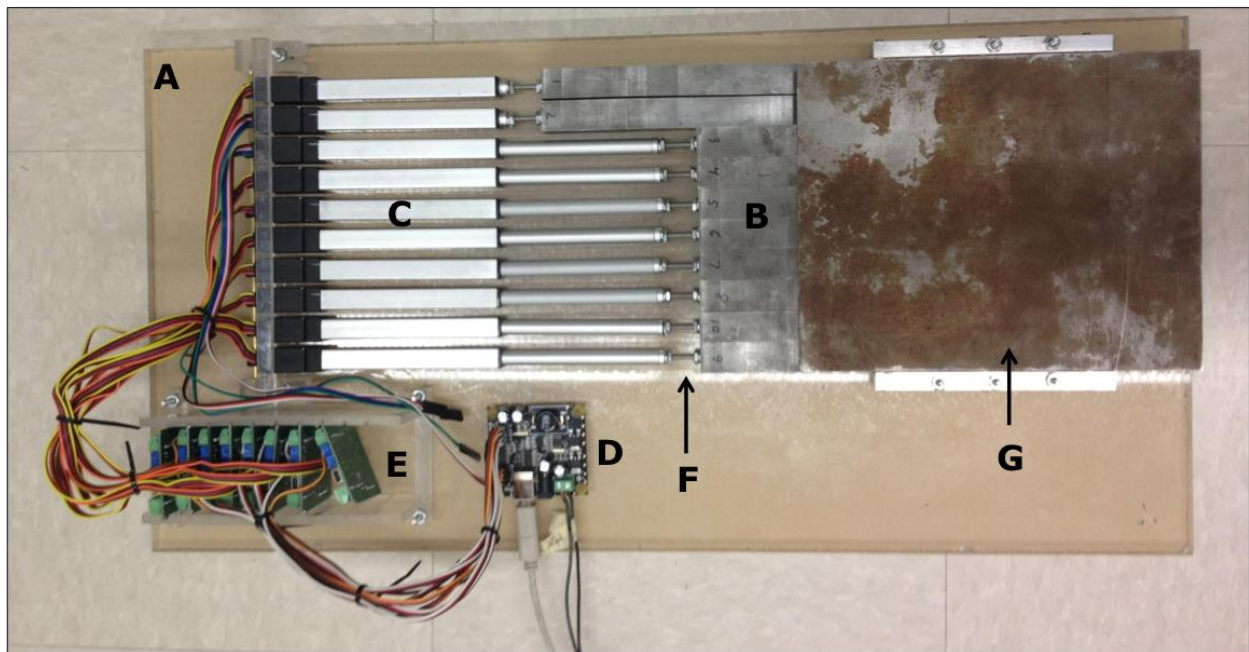


Figure 14: The final device, which can be used to dynamically attenuate X-Rays to a patient on the Siemens Artis Zeego C-Arm CT.

The motor controller is run with a Java program that inputs a formatted text file with required position of each motor, based on the required regional thickness, and translates that information to motor pulses. The Java code can be found in Appendix E: Java Code.

TESTING

A Test Plan was developed and carried out to better examine the properties of the Firgelli L-12 I and Firgelli L-12 P Linear Servomotors. The Test Plan can be found in Appendix C. As stated in the Test Plan, testing included several forms of position testing.

Positional Accuracy and Precision Testing using Calipers

As the motor used to drive the wedge requires precise positional accuracy and precision, these qualities of the L-12 I and P Linear Servomotors were determined in order to compare the actual motor characteristics to the characteristics listed in the datasheet. Our client wishes to send each wedge to multiple positions during the scan, which makes it necessary to have precise wedge positioning at all times. Precision is important because the wedge must achieve an accurate position to correctly attenuate the X-Ray beam.

Positional accuracy and precision were tested by moving the motor to randomly generated positions and measuring the distance travelled with a caliper. The wedges were tested while resting on a flat surface and guided using the linear track attached to the bottom of a wedge. To prevent measurement inaccuracies caused by accidental wedge movement, the distance measured was the distance between the wedge and the motor housing; this distance was determined by servo arm movement and therefore was the actual distance travelled by the wedge. Thirty different positions were generated and the distance values were recorded for each position. A linear relationship was obtained between the distance travelled and the wedge position input and an r^2 value generated for the linear relationship. The results can be found in Figure 15. Additional calculations determined the wedges can be reliably positioned within 180 microns of the value predicted in the linear relationship. This value is under the 200 micron position standard deviation given in the L12 I and L12 P datasheets.

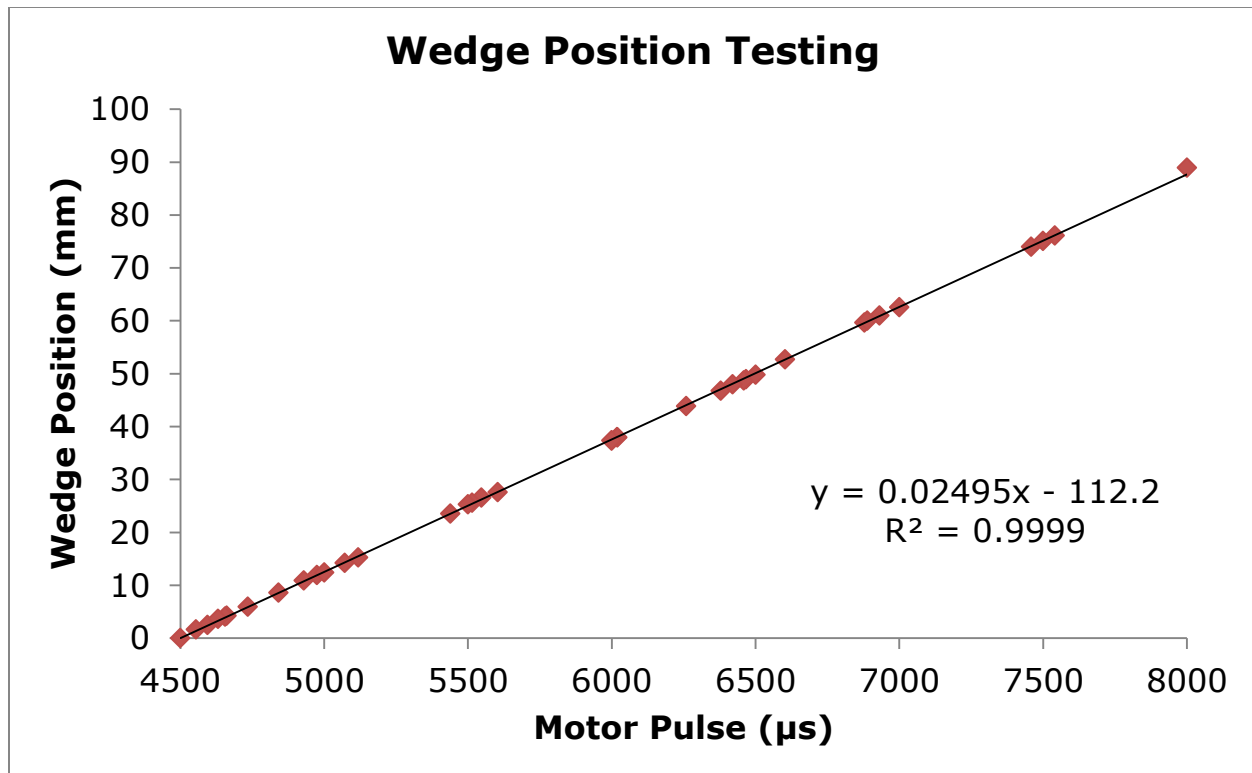


Figure 15: Wedge position as a function of input pulse. The wedge can be reliably positioned within 180 microns of the predicted position using this linear relationship.

Positional Accuracy and Precision Testing using CT Scanner

To further evaluate the reproducibility of wedge positions, additional position testing was carried out using the Siemens Artis Zeego C-Arm CT scanner. The wedges were placed in known positions and imaged, then moved to random positions, moved back, and re-imaged. If the wedges did not return to the same positions each time, the images would be different and the difference would be evident after image analysis.

Different CT images were compared using image subtraction techniques. In this technique, the value of each pixel in one image is subtracted from the value of that same pixel in another image. If two identical CT images were subtracted, the image is expected to have no distinguishable characteristics and be filled with random noise. As seen in Figure 16 on the following page, six of the wedges are distinguishable in image (A) but none of the wedges are distinguishable in (B). This is due to the high similarity between the two images used to create image (B) using image subtraction.

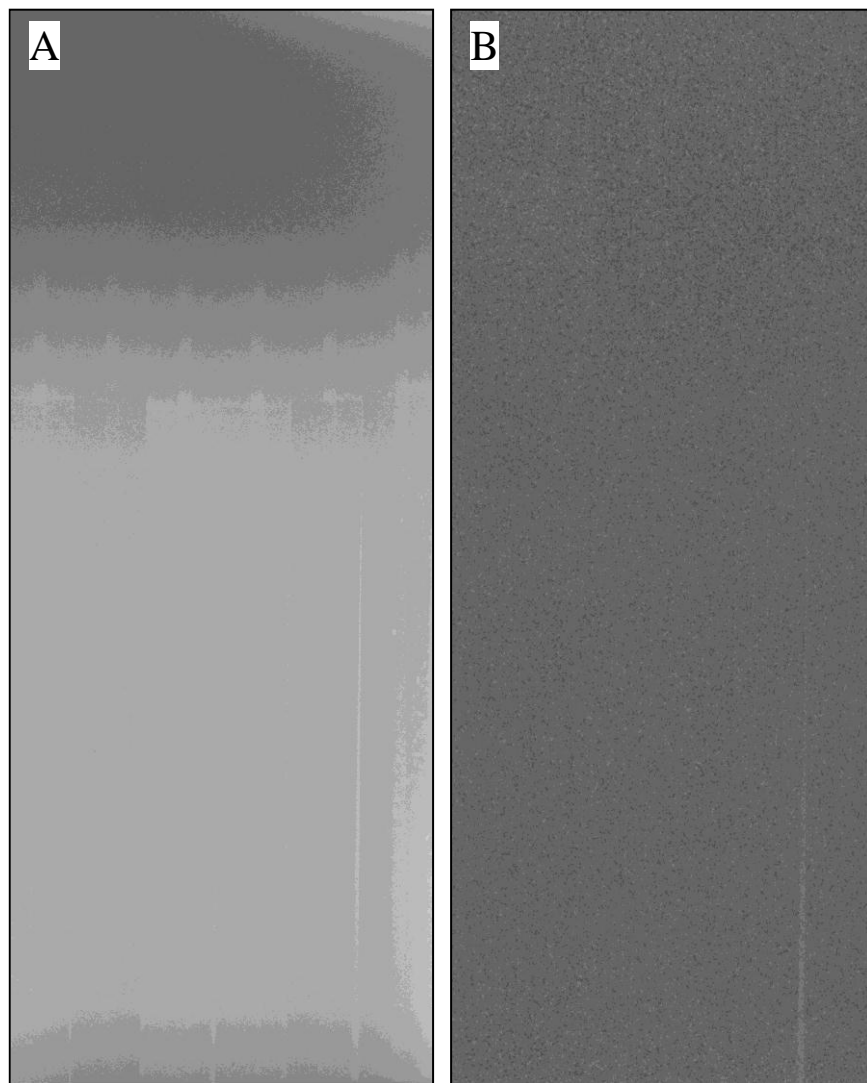


Figure 16:
(A): Image of six wedges.
(B): Representative image obtained after two images were subtracted.

The amount by which two images differ can be found by taking the mean of the pixel values in a subtracted image. In a CT subtracted image, if the two images used were identical the expected mean is zero. After performing the analysis described in the Test Plan and comparing all the subtracted images, we found that the average difference between two CT images was $0.12 \pm 0.079\%$. This small value indicates that the two images, taken before and after wedge movement, are very similar, and allows us to infer that the wedges can be positioned with a high degree of repeatability.

ERGONOMICS

The International Ergonomics Association has defined ergonomics as “the understanding of interactions among humans and other elements of the system in order to optimize human well-being and overall system performance” [17]. This prototype is a proof of concept to Siemens, so that this device could potentially be built within a future CT machine. Since there will be no human interface with this device, there are no major ergonomic factors.

ETHICAL CONSIDERATIONS

The main ethical consideration for this project is that no harm comes to the patient or the doctor during the duration of the procedure. If the design were to be implemented into future CT scanners, it must remain relatively light in weight and fastened securely so the device does not move as the scanner revolves quickly around the patient. This would ensure that the calibration of the scanner is not effected, and that there is no risk of the device coming loose. However, the prototype will only be used as a proof of concept and will not be implemented within the scanner. Instead, it will be fashioned to a table as an object is revolved to simulate an actual scan. Because of this, there are no major ethical considerations for the scope of this prototype.

FUTURE WORK

Testing

The next phase of prototype testing will involve the use of a CT phantom (a phantom is an object used to mimic a patient or an imaging task found in real patients), which will be used to evaluate the dose reduction, signal to noise improvement, and scatter reduction using quantitative metrics. Testing will be performed at the Wisconsin Institute for Medical Research using the available Siemens Artis Zeego C-Arm CT machine. Simulations run in MATLAB showed a dose reduction up to 43% in certain areas of the patient, up to a 9% increase in signal to noise ratio, and a reduction in scatter of up to 79%. The data received from phantom testing will allow for comparisons between the MATLAB simulations and physical device performance.

Patenting

A similar concept to our design was patented within the past year under US Patent 7,893,412 B2 and describes a generic dynamic attenuating system. However, the concept was not

optimized for use with CT scanners, does not vary attenuation spatially with time, and consists of a single attenuating element. The novelty of our design includes optimized metal composition and size, multiple track-guided attenuating elements, and the ability to provide real-time position feedback during the scan. This prompted our client to apply for a patent early in the design development, which is currently still pending.

Marketing

The project is currently sponsored by Siemens, and once the testing and patenting processes are completed, the design will be presented to them along with quantitative dose reduction, signal to noise improvement, and scatter reduction metrics. Ideally, Siemens will perform additional research into reducing the device size and increasing overall performance before integrating a form of the device into a future generation of CT technology. In the next five years, the US healthcare imaging and therapy systems market is estimated to quintuple. Siemens currently holds 36% of the market share in healthcare imaging and therapy systems, which would facilitate market penetration and decrease the time to market for the dynamic beam attenuator. If implemented, the device would improve patient safety and image quality, reduce the number of cancers caused by CT scans, and increase a clinician's diagnostic efficiency.

REFERENCES

- [1] D. Brenner, "Slowing the Increase in the Population Dose Resulting from CT Scans," *Radiation Research*, vol. 174, no. 6b, pp. 809-815, 2010.
- [2] C. Mistretta, "Mistretta, Charles A.," 19 August 2011. [Online]. Available: http://www.engr.wisc.edu/bme/faculty/mistretta_charles.html.
- [3] The Board of Regents of the University of Wisconsin, "Dr. Charles Mistretta," 2011. [Online]. Available: <https://www.radiology.wisc.edu/people/facultyContent.php?vaultID=69>.
- [4] Siemens AG, "Artis Zeego," 2012. [Online]. Available: http://www.medical.siemens.com/webapp/wcs/stores/servlet/ProductDisplay~q_catalogId~e_-1~a_catTree~e_100000~a_langId~e_-1~a_productId~e_181902~a_storeId~e_10001.htm.
- [5] R. Ketcham, "X-Ray Computed tomography (CT)," 1 February 2011. [Online]. Available: http://serc.carleton.edu/research_education/geochemsheets/techniques/CT.html. [Accessed 25 February 2012].
- [6] "The Nobel Prize in Physiology or Medicine 1979," 2012. [Online]. Available: http://www.nobelprize.org/nobel_prizes/medicine/laureates/1979/.
- [7] Siemens Medical, "CT History and Technology," [Online]. Available: http://www.medical.siemens.com/siemens/zh_CN/gg_ct_FBAs/files/brochures/CT_History_and_Technology.pdf. [Accessed 27 February 2012].
- [8] A. Kak and M. Slaney, *Principles of Computerized Tomographic Imaging*, IEEE Press, 1988.
- [9] L. Goldman, "Principles of CT and CT Technology," *Journal of Nuclear Medicine Technology*, vol. 35, no. 3, pp. 115-128, 2007.
- [10] U.S. Food and Drug Administration, "Computed Tomography (CT)," 9 November 2010. [Online]. Available: <http://www.fda.gov/Radiation-EmittingProducts/RadiationEmittingProductsandProcedures/MedicalImaging/MedicalX-Rays/ucm115317.htm>.
- [11] T. Szczykutowicz and C. Mistretta, "Practical considerations for intensity modulated CT," *Proceedings of SPIE Medical Imaging*, vol. 8313, no. 161.
- [12] W. Kalender, H. Wolf and C. Suess, "Dose reduction in CT by anatomically adapted tube current modulation. II. Phantom measurements," *Medical physics*, vol. 26, p. 2248, 1999.
- [13] S. Lee, S. Yoon, S. Yoo, Y. Ji, K. Kim, S. Kim and J. Lee, "comparison of image quality and radiation dose between combined automatic tube current modulation and fixed tube current technique in CT of abdomen and pelvis," *Acta Radiologica*, vol. 52, no. 10, pp. 1101-1106, 2011.
- [14] C. H. McCollough, M. R. Bruesewitz and J. J. Kofler, "CT Dose Reduction and Dose

- Management Tools: Overview of Available Options," *RadioGraphics*, vol. 32, no. 1, pp. 503-512, 2006.
- [15] F. Faulhaber, "Linear DC-Servomotors with Analog Hall Sensors QUICKSHAFT(R) Technology," 2012. [Online]. Available: http://www.micromo.com/Micromo/LinearDCServomotors/LM_1247-01_MIN.pdf. [Accessed 13 March 2012].
- [16] J. G. Webster, *Medical Instrumentation: Application and Design.*, Wiley, 1997.
- [17] "Definition of Ergonomics," International Ergonomics association, 31 August 2011. [Online]. Available: http://www.iea.cc/01_what/What is Ergonomics.html. [Accessed 2011 October 19].
- [18] F. Faulhaber, "Brushless DC Servomotors," Micromo Micro Motion Solutions, 2012. [Online]. Available: <http://www.micromo.com/brushless-dc-servomotors.asp>. [Accessed 13 March 2012].
- [19] "What is EDM and the advantages of using it?," Wire-Cut Technologies Ltd., 2012. [Online]. Available: <http://www.wire-cut.co.uk/wireedm.htm>. [Accessed March 13 2012].
- [20] Universal Medical Inc., "CT Phantoms," Volusion, 2012. [Online]. Available: <http://www.universalmedicalinc.com/CT-Phantoms-s/304.htm>. [Accessed 13 March 2012].
- [21] U.S. Food and Drug Administration, "Computed Tomography (CT)," 09 November 2010. [Online]. Available: <http://www.fda.gov/Radiation-EmittingProducts/RadiationEmittingProductsandProcedures/MedicalImaging/MedicalX-Rays/ucm115317.htm>. [Accessed 29 September 2011].
- [22] Nobel Prize, "Physiology or Medicine 1979 - Press Release," [Online]. Available: http://www.nobelprize.org/nobel_prizes/medicine/laureates/1979/press.html. [Accessed 12 October 2011].
- [23] A. Kak and M. Slaney, *Principles of Computed Tomographic Imaging*, IEEE Press, 1988.
- [24] R. Ketcham, "X-Ray Computed Tomography (CT)," 1 February 2011. [Online]. Available: http://serc.carleton.edu/research_education/geochemsheets/techniques/CT.html. [Accessed 29 September 2011].
- [25] C. H. McCollough, M. R. Bruesewitz and J. M. Kofler, "CT Dose Reduction and Dose Management Tools: Overview of Available Options," *RadioGraphics*, 2004.
- [26] C. Mistretta, "Mistretta, Charles A.," 19 August 2011. [Online]. Available: http://www.engr.wisc.edu/bme/faculty/mistretta_charles.html.
- [27] T. B. o. R. o. t. U. o. W. System, "Dr. Charles Mistretta," 2011. [Online]. Available: <https://www.radiology.wisc.edu/people/facultyContent.php?vaultID=69>.
- [28] MICROMO, "Micro Drive Solutions," 2011. [Online]. Available: <http://www.micromo.com>. [Accessed 29 September 2011].
- [29] R. Condit, "Brushed DC Motor Fundamentals," 26 January 2004. [Online]. Available: <http://ww1.microchip.com/downloads/en/AppNotes/00905a.pdf>. [Accessed 13 September 2011].

- [30] R. Condit and D. W. Jones, "Stepping Motors Fundamentals," 26 January 2004. [Online]. Available: <http://ww1.microchip.com/downloads/en/AppNotes/00907a.pdf>. [Accessed 13 September 2011].
- [31] Schneider Electric, "MDrive 23 Datasheet," [Online]. Available: <http://imshome.com/downloads/datasheets/MLM23.pdf>. [Accessed 7 December 2011].
- [32] J. Xia and W. K. Durfee, "Analysis of Small-Scale Hydraulic Systems," *IEEE Trans. Mechatronics*, 2011.
- [33] Figrelli Technologies, Inc., "L16 Series Datasheet," 2011. [Online]. Available: http://www.firgelli.com/Uploads/L16_datasheet.pdf. [Accessed 17 September 2011].
- [34] Schneider Electric, "M Drive Plus 17 Linear Actuator Datasheet," [Online]. Available: <http://imshome.com/downloads/datasheets/MLM17.pdf>. [Accessed 12 December 2011].
- [35] Schneider Electric, "M Drive Plus 14 Linear Actuator Datasheet," [Online]. Available: <http://imshome.com/downloads/datasheets/MLM14.pdf>. [Accessed 12 December 2011].
- [36] Micromo, "2-Phase Stepper Motors," 8 June 2011. [Online]. Available: http://www.micromo.com/datasheets/Stepper%20Motors/ADM_0620_PCS.pdf. [Accessed 7 December 2011].
- [37] Micromo, "QUICKSHAFT Technology," 2011. [Online]. Available: http://www.micromo.com/datasheets/Linear%20Motors/LM_0830-01_MIN.pdf. [Accessed 7 December 2011].
- [38] R. e. a. Gupta, "Flat-Panel Volume CT: Fundamental Principles, Technology, and Applications," *RadioGraphics*, pp. 2009-2022, 2008.
- [39] Phidgets, "Product Manual: 1061 - PhidgetAdvancedServo 8-Motor," 2012. [Online]. Available: http://www.phidgets.com/documentation/Phidgets/1061_1_Product_Manual.pdf. [Accessed 12 April 2012].
- [40] G. Housenfeld, "Computerized transverse axial scanning (tomography): Part i. description of system," *British Journal of Radiology*, vol. 46, pp. 1016-1022, 1973.
- [41] C. Lee, J. Goo, H. Ye, S. Ye, C. Park, E. Chun and J. Im, "Radiation dose modulation techniques in the multidetector ct era: From basics to practice," *Radiographics*, vol. 28, no. 5, p. 1451, 2008.
- [42] D. Leswick, M. Hunt, S. Webster and D. Fladeland, "Thyroid shields versus z-axis automatic tube current modulation for dose reduction at neck ct1," *Radiology*, vol. 249, no. 2, p. 572, 2008.
- [43] J. Li, S. Woloschek, T. Toth and J. Schmidt, "Method and apparatus of ct imaging with voltage modulation". United States of America Patent 6,836,529, 28 December 2008.
- [44] S. Graham, D. Moseley, J. Siewerdsen and D. Jaffray, "Compensators for dose and scatter management in code-beam computed tomography," *Medical physics*, vol. 24, p. 2691, 2007.

- [45] W. Kalender, *Computed tomography: fundamentals, system technology, image quality, applications*, Wiley-VCH, 2000.
- [46] T. Buzug, *Computed tomography: from photon statistics to modern cone-beam CT*, Verlag: Springer, 2008.
- [47] J. Hsieh, *Computed tomography: principles, design, artifacts, and recent advances*, Society of Photo Optical, 2003.
- [48] T. Mackie, T. Holmes, S. Swerdloff, P. Reckwerdt, J. Deasy, J. Yang, B. Paliwal and T. Kinsella, "Tomotherapy: a new concept for the delivery of dynamic conformal radiotherapy," *Medical Physics*, vol. 20, no. 6, pp. 1709-1719, 1993.
- [49] K. Ruchala, G. Olivera, J. Kapatoes, E. Schloesser, P. Reckwerdt and T. Mackie, "Megavoltage CT image reconstruction during tomotherapy treatments," *Physics in Medicine and Biology*, vol. 45, p. 3545, 2000.
- [50] K. Ruchala, G. Olivera, E. Schloesser and T. Mackie, "Megavolt CT on a tomotherapy system," *Physics in Medicine and Biology*, vol. 44, p. 2597, 1999.

APPENDIX A – MATLAB CODE

```

kV = [1:150];
sigPatient = sum(kV.*phi_tube100.*exp(-muBone*1 - muSoftTissue*36));

meanEPatient = sigPatient/sum(phi_tube100.*exp(-muBone*1 - muSoftTissue*36));

t = zeros(1,92);
meanELeaf = zeros(1,92);
for z=1:92

    func = @(x)-sigPatient+sum(kV.*phi_tube100.*exp(-A{z,1}(1:150,9)*density(z,2)*x(1)));
    t(z) = fzero(func,[-0.0001 260000000]);
    meanELeaf(z) = sum(kV.*phi_tube100.*exp(-
A{z,1}(1:150,9)*density(z,2)*t(z)))/sum(phi_tube100.*exp(-
A{z,1}(1:150,9)*density(z,2)*t(z)));
end

figure;semilogy(t);
figure;plot(meanELeaf - meanEPatient);

```

```

muAl = A{13,1}(1:150,9)*density(13,2);
muFe = A{26,1}(1:150,9)*density(26,2);
muW = A{74,1}(1:150,9)*density(74,2);
muCu = A{29,1}(1:150,9)*density(29,2);
muPb = A{82,1}(1:150,9)*density(82,2);

muBone =
muRhoCompound{spektrCompound2C('Bone'),1}(1:150,9)*densityCompounds(spektrCompound2C('Bone'));
muSoftTissue =
muRhoCompound{spektrCompound2C('SoftTissue'),1}(1:150,9)*densityCompounds(spektrCompound2C('SoftTissue'));

figure;semilogy(1:150,muAl,'--',1:150,muBone,'-');xlabel('Energy (keV)');ylabel('Linear Attenuation Coefficients (cm^{-1})');zlabel('Path Length (cm)');
title('Linear Attenuation Coefficients');
hold on
semilogy(1:150,muFe,'--r');
semilogy(1:150,muW,'--m');
semilogy(1:150,muCu,'--c');
semilogy(1:150,muPb,'--k');
semilogy(1:150,muSoftTissue,'-r');
legend('Aluminum', 'Bone', 'Iron', 'Tungsten', 'Copper', 'Lead', 'Soft Tissue');
hold off

```

APPENDIX B – PROJECT DESIGN SPECIFICATIONS

Digital Beam Attenuator (Beam Attenuator)
Project Design Specifications
02/06/2012

Group Members: Michael Scherer, Katherine Lake, Clara Chow, Ashley Mulchrone

Advisor: Professor Paul Thompson

Clients: Dr. Charles Mistretta and Timothy Szczykutowicz, Medical Physics

Problem Statement: In X-Ray Computed Tomography, a uniform X-Ray beam is used despite the fact that the transmission through the patient varies significantly due to the patient's anatomy. For almost any clinical or proposed medical x-ray imaging system, either a proposal for intensity modulation (IM) exists in literature or a form of IM is implemented clinically, but these forms of IM are limited in that they cannot adapt the incident photon flux over time to match all projections. The use of a uniform X-Ray incident beam results in a non-uniform signal-to-noise ratio, a sub-optimal distribution of X-Ray scatter, and significantly higher or lower dose than necessary to some regions of the body. Since current devices are only able to statically attenuate the X-Ray beam, we propose to design and actuate a series of dynamically attenuating wedge pairs placed between the X-Ray source and the patient. The attenuating wedges will use the changing thickness of the wedge pairs to locally attenuate the incident beam, which will result in improved image quality and reduced X-Ray dosages.

Client Requirements:

- A new prototype shall be designed and manufactured.
- The system shall linearly actuate the prototype.
- The wedges of the prototype shall move in response to pre-programmed positions.
- The wedges of the prototype shall move independently.

1. Physical and Operational Characteristics

- A. Performance requirements:** The device shall alter the strength of the X-Ray beam as a function of position for the duration of the Computed Tomography (CT) scan. The device must move at a minimum speed of 15 mm/s. The prototype must actuate the wedges to satisfy a dynamic range that encompasses the entire X-Ray beam.
- B. Safety:** The prototype must not be harmful to the researcher, user, or patient. The prototype must not harm the machine or interfere with its intended operation. It also must be self-contained during the duration of the scan.
- C. Accuracy and Reliability:** The actuator must be able to move the wedges within 1 mm of accuracy.
- D. Life in Service:** The device will be a prototype and thus has a limited life in service. The device shall have a life in service of one year of frequent use. If implemented clinically, the device must have a life in service equal to that of the CT scanner.

- E. Operating Environment:** The prototype is to be used by graduate students and professor in a CT research lab. During testing, the device will be exposed to X-Ray radiation; therefore, design components must be resistant to X-Ray damage.
- F. Ergonomics:** There are no ergonomic concerns relating to the prototype.
- G. Size:** The prototype shall be as small as possible while maintaining full functionality. It must be large enough to attenuate the X-Ray beam throughout the entire dynamic range at a minimum of 31.75 cm from the X-Ray point source.
- H. Weight:** The prototype shall be as lightweight as possible while maintaining an appropriate level of X-Ray attenuation.
- I. Materials:** All parts shall be resistant to damage by X-Ray radiation. The wedge material shall be homogeneous in order to uniformly transmit X-Rays and correctly attenuate the X-Ray beams. It shall also slide with a low coefficient of friction.
- J. Aesthetics, Appearance, and Finish:** The device is a prototype and therefore functionality is the dominant consideration over aesthetics and appearance.

2. Production Characteristics

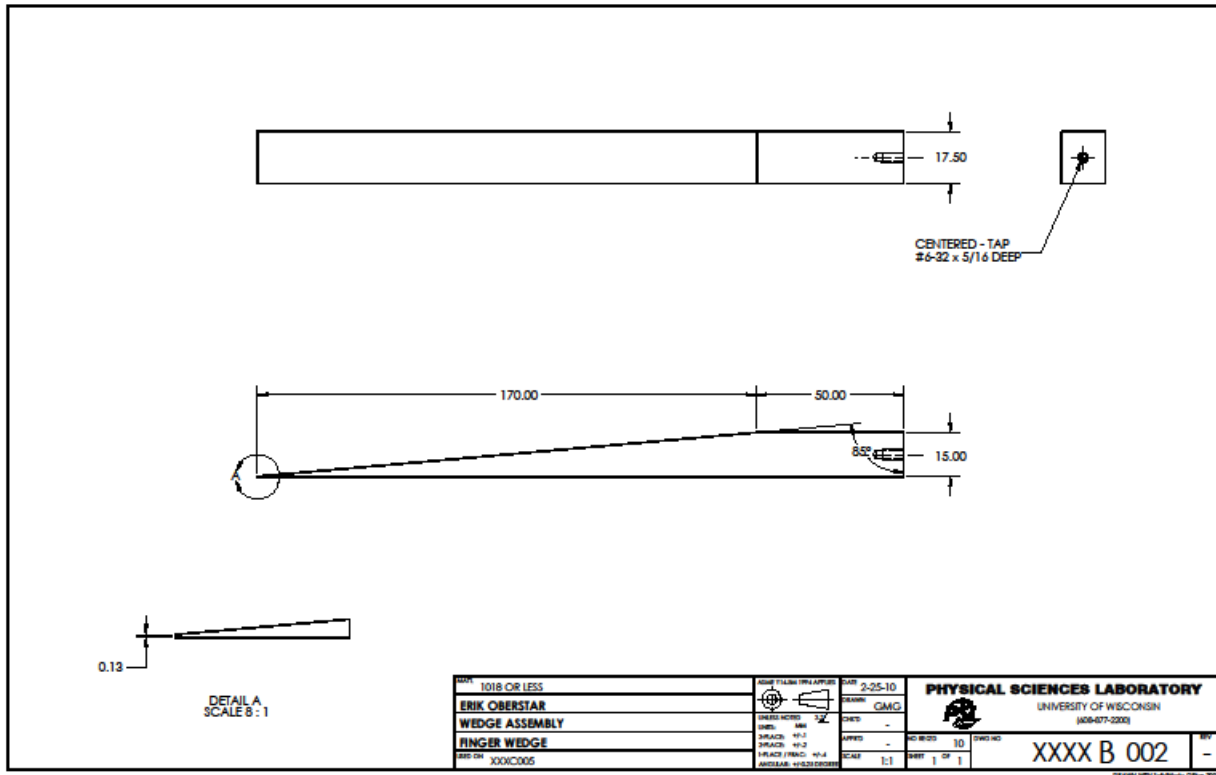
- A. Quantity:** One prototype shall be produced.
- B. Target Product Cost:** The budget for this semester is \$5,000.

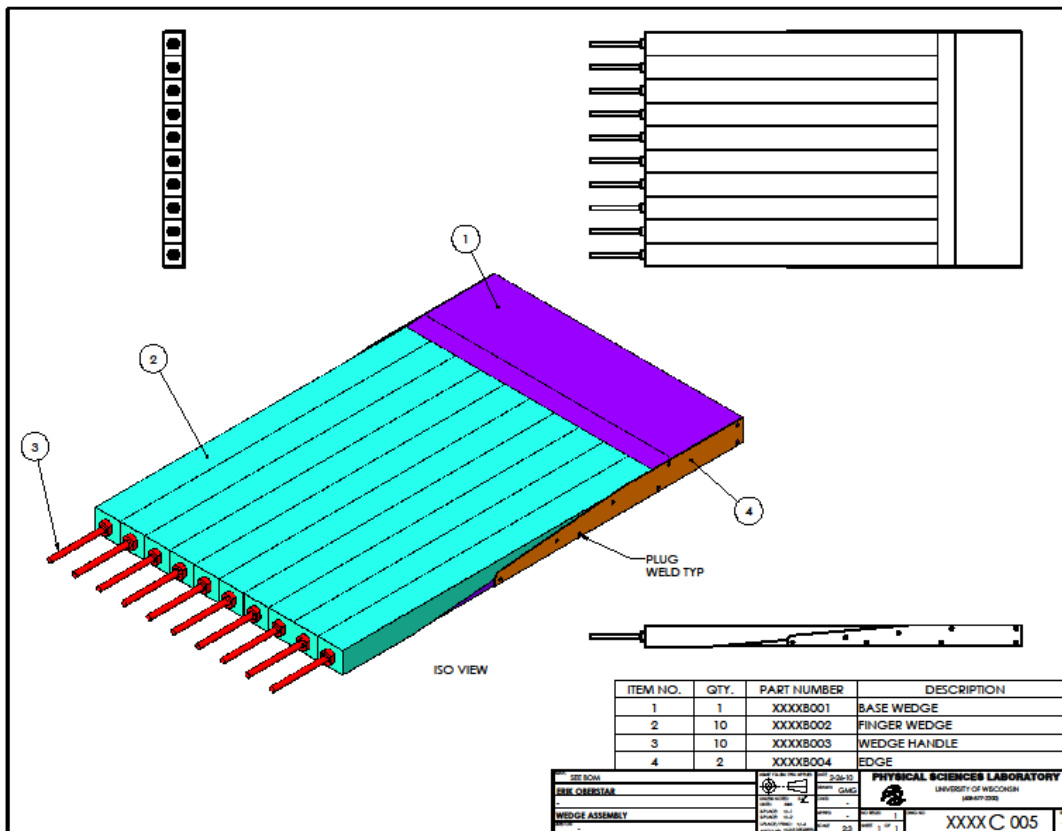
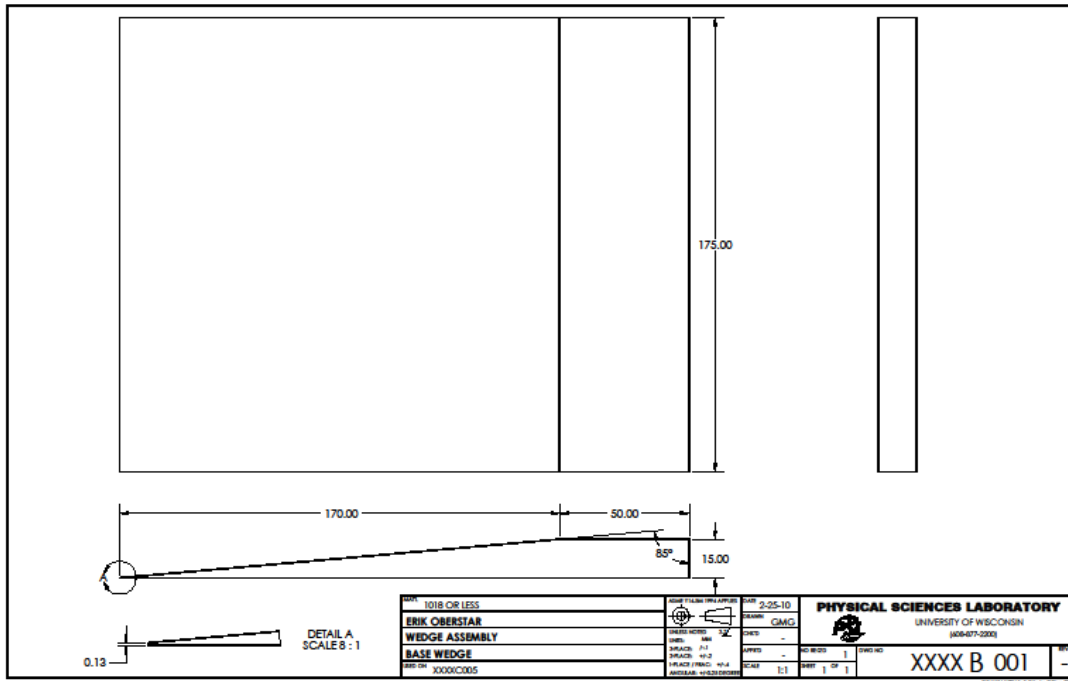
3. Miscellaneous

- A. Standards and Specifications:** The final product will require the approval of the Food and Drug Administration and clinical trials. The prototype is a proof of concept and therefore will not require government approval.
- B. Customer:** The intended user is a medical professional or researcher who will utilize Digital Beam Attenuation to improve CT image quality during a medical procedure or for diagnostic purposes.
- C. Patient-related Concerns:** As our design may eventually be commercially available for medical professional use, it should follow all restrictions enforced by the Food and Drug Administration. It must not cause any harm to its user.
- D. Competition:** No other forms of Digital Beam Attenuation exists at this time. Statistical CT image Reconstruction is also being used to create better quality CT images, but that technology is currently in development. In addition, static devices like bowtie filters are currently being used to attenuate X-Ray beams on CT scanners.

APPENDIX C: TECHNICAL DRAWINGS

Appendix A, made up of the following two pages, consists of technical drawings of the prototype provided to the team by Erick Oberstar. These technical drawings are detailed schematics of the prototype.





APPENDIX D: TEST PLAN

Introduction

This test approach document describes the appropriate strategies and processes used to plan, organize, and execute testing of the digital beam attenuator project actuated wedges.

Quality Objective

1.1.1 Primary Objective

The primary objective of testing this system is to ensure it meets the full requirements, including the quality requirements, provided by the client. The system shall satisfy the use case scenarios and maintain the quality of the project. At the end of the design project, the client should find that the project has met or exceeded all of their expectations as detailed in the requirements.

1.2.1 Secondary Objective

The secondary objective of testing the digital beam attenuator actuation system is to identify and expose all issues and associated risks, communicate discovered issues to the design team, and ensure that all issues are addressed prior to the completion of the design project. All areas of the system must be examined and all issues found must be documented and dealt with appropriately.

Test Methodology

2.1 Purpose

The purpose of the Test Plan is to achieve the following:

- Define strategies to test all the functional and quality requirements.
- Identify required resources and related information.
- Define data capture and analysis methods.
- Ensure sufficient test documentation to allow test reproducibility.

2.2 Test Strategies

2.2.1 Position Test using Calipers

The purpose of this test is to determine the accuracy and precision of the motor.

The test shall be conducted as follows:

- Connect the motor to the wedge via the adapter.
- Send the motor a command that causes it to move to a randomly generated point.
- Measure the distance the wedge travelled by measuring the distance between the body of the motor and the back of the wedge. This will remove any inaccuracies caused by the motor moving the test and displacing the wedge from its initial position.
- Record the position input and the distance travelled using calipers.
- Use $n = 30$ trials and generate a new random position each time.

Analysis of the positions shall be conducted as follows:

- Plot the motor position versus the randomly generated point for each of the commands.
- Create a linear trend line to determine the expected motor position at each position input value.
- Find the r^2 value of the trend line.
- Calculate each point's deviation from the expected position on the trend line.
- Use the deviation to calculate the standard deviation of wedge positions

All values shall be recorded in a Microsoft Excel spreadsheet.

2.2.2 Position Test using Computed Tomography (CT) Scanner

The purpose of this test is to determine the repeatability of wedge positioning.

The test shall be conducted as follows:

- Connect each wedge to a motor.
- Set the wedges to a known initial position.
- Take a CT image of the wedges.
- Move each wedge to a randomly generated point.
- Return each wedge to the known initial position.
- Take a CT image of the wedges.
- Subtract the two images using ImageJ to generate a subtracted image.

Analysis of the subtracted image shall be conducted as follows:

- Crop image to uniform size.
- Obtain the mean pixel value for subtracted image and for original images.
- Average mean pixel values for subtracted images and for original images.
- Calculate standard deviation of mean pixel values.
- Determine the ratio of mean pixel value for subtracted images to mean pixel values for original images.

APPENDIX E: JAVA CODE

Appendix E contains the java code for the PhidgetAdvancedServo 8-Motor servo controller. The code was created in Java Eclipse Version: Indigo Service Release 1Build id: 20110916-0149. Proper code function requires the use of the phidget21.jar file, which can be found on the PhidgetAdvancedServo 8-Motor servo controller website.

Servo Controller Class

```
import java.io.BufferedReader;
import java.io.FileReader;

import com.phidgets.AdvancedServoPhidget;
import com.phidgets.Phidget;
import com.phidgets.event.ErrorEvent;
import com.phidgets.event.ErrorListener;

/**
 * A class that controls the PhidgetAdvancedServo 8-Motor Controller using a
 * text file as an input.
 *
 * @author Katherine Lake
 */
public class FilePhidgetServoController
{
    public static final void main(String args[]) throws Exception
    {
        // Creates a new servo object
        AdvancedServoPhidget servo;

        // Inputs the file name from the command line argument
        // EX: commandfile.txt
        if (args.length != 1)
        {
            // If this error occurs, check that your file is in the 'Phidget'
            // folder (at the same level as src, Referenced libraries, etc
            // Also check you typed the file name correctly and that it also
            // has .txt at the end of it
            System.err.println("Usage: PhidgetServoController <filename>");
            return;
        }
        String commandFilename = args[0];

        System.out.println(Phidget.getLibraryVersion());
        // Instantiates a new phidget object
        servo = new AdvancedServoPhidget();

        // This will print out errors if there are any. Check the Phidget
        // documentation and API if errors occur
        servo.addErrorListener(new ErrorListener()
        {
            public void error(ErrorEvent ee)
            {
                System.out.println("error event for " + ee);
            }
        });
    }
}
```

```

// Opens any servos that the controller sees.
servo.openAny();
System.out.println("waiting for AdvancedServo attachment...");
servo.waitForAttachment();

// Print the serial port connection and the number of motors
System.out.println("Serial: " + servo.getSerialNumber());
System.out.println("Servos: " + servo.getMotorCount());

// Open the command file
BufferedReader reader =
    new BufferedReader(new FileReader(commandFilename));
// Read each line of the command file
String line;
while ((line = reader.readLine()) != null)
{
    // Truncate the line at the comment character
    int index = line.indexOf('#');
    if (index != -1)
    {
        line = line.substring(0, index);
    }
    // Trim and preceding or trailing whitespace
    line = line.trim();

    // Skip blank lines
    if (line.isEmpty())
    {
        continue;
    }

    // Split the line into tokens on white space
    String[] tokens = line.split("\\s+");

    // Read the command
    String command = tokens[0];
    if (command.equalsIgnoreCase("engage"))
    {
        // This will engage the servo
        // Each of the servos must be engaged before they can be moved
        int servoIndex = Integer.parseInt(tokens[1]);
        System.out.println("engage(" + servoIndex + ")");
        servo.setEngaged(servoIndex, true);
        servo.setSpeedRampingOn(servoIndex, false);
        System.out.println("Servo index " + servoIndex
            + " engaged and speed ramping off.");
    } else if (command.equalsIgnoreCase("setPosition"))
    {
        // Set the servo position
        int servoIndex = Integer.parseInt(tokens[1]);
        double position = Double.parseDouble(tokens[2]);
        System.out.println("setPosition(" + servoIndex + ", "
            + position + ")");
        servo.setPosition(servoIndex, position);
    } else if (command.equalsIgnoreCase("sleep"))
    {
        // Sleep the servo
        // This command must occur after every movement command
    }
}

```

```

        int time = Integer.parseInt(tokens[1]);
        System.out.println("sleep(" + time + ")");
        Thread.sleep(time);
    } else
    {
        System.err.println("Unknown command: " + command);
        continue;
    }
}
// Close the servo and the buffered reader - must be closed!!!
servo.close();
reader.close();
System.out.println("Done");
}
}

```

Test Code Generator Class

```

import java.util.Random;
import java.io.*;
/**
 * A class that generates psuedorandom positions and writes them to a text file.
 * For use with FilePhidgetServocontroller class.
 *
 * @author Katherine
 *
 */
public class TestCodeGenerator
{
    // number of servos - to change code, change this constant first
    public static final int NUM_SERVOS = 8;
    // number of positions you want the code to generate
    public static final int NUM_POSITIONS = 1;
    public static void main(String args[])
    {
        // Random number object - to generate the same random numbers each time,
        // 'seed' (start) the random object with a number - ie Random(4);
        // instead of Random(); . Random(); seeds the random generator with a
        // number from the computer's clock
        Random rng = new Random();
        // Create a new PrintStream object
        PrintStream out;
        // Must surround instantiating object with 'try-catch block' - used in
        // error handling.
        try
        {
            // Create a new file or find the file called "commands.txt"
            out = new PrintStream(new FileOutputStream("commands.txt"));
            // Print a header to the file
            out.println("#Randomly generated test code for FilePhidgetServoController.java
                \n");

            // Engage each servo - required for Phidget. Comment out if using
            // this code for maestro controller
            for (int servo = 0; servo < NUM_SERVOS; servo++)
            {
                out.println("engage " + servo);
            }
            // Generate random positions for each servo
            for (int pos = 1; pos <= NUM_POSITIONS; pos++)
            {

```

